Cell Metabolism
Article

Tyk2 and Stat3 Regulate Brown Adipose Tissue Differentiation and Obesity

Marta Derecka,[1] Agnieszka Gornicka,[2] Sergei B. Koralov,[3] Karol Szczepanek,[1] Magdalena Morgan,[1] Vidisha Raje,[1] Jennifer Sisler,[1] Qifang Zhang,[1] Dennis Otero,[4] Joanna Cichy,[5] Klaus Rajewsky,[6] Kazuya Shimoda,[7] Valeria Poli,[8] Birgit Strobl,[9] Sandra Pellegrini,[10] Thurl E. Harris,[11] Patrick Seale,[12] Aaron P. Russell,[13] Andrew J. McAinch,[14] Paul E. O'Brien,[15] Susanna R. Keller,[16] Colleen M. Croniger,[17] Tomasz Kordula,[1] and Andrew C. Larner[1,*]

[1]Department of Biochemistry and Molecular Biology and Massey Cancer Center, Virginia Commonwealth University, Richmond, VA 23298, USA
[2]Department of Immunology, Cleveland Clinic Foundation, Cleveland, OH 44195, USA
[3]Department of Pathology, New York University Medical School, New York, NY 10016, USA
[4]Division of Biological Sciences, University of California, San Diego, La Jolla, CA 92093, USA
[5]Department of Immunology, Faculty of Biochemistry, Biophysics, and Biotechnology, Jagiellonian University, 30-387 Krakow, Poland
[6]Program in Cellular and Molecular Medicine, Children Hospital, and Immune Disease Institute, Harvard Medical School, Boston, MA 02115, USA
[7]Department of Gastroenterology and Hematology, Faculty of Medicine, University of Miyazaki, 5200 Kihara, Kiyotake, Miyazaki 889-1692, Japan
[8]Department of Genetics, Biology, and Biochemistry, Molecular Biotechnology Center, University of Turin, Via Nizza 52, 10126 Torino, Italy
[9]Institute of Animal Breeding and Genetics, Department for Biomedical Sciences, University of Veterinary Medicine Vienna, 1210 Vienna, Austria
[10]Department of Immunology, Institut Pasteur, 25–28 Rue du Docteur Roux, 75724 Paris, France
[11]Department of Pharmacology, University of Virginia School of Medicine, Charlottesville, VA 22903, USA
[12]Department of Cell and Developmental Biology, University of Pennsylvania School of Medicine, Philadelphia, PA, 19104, USA
[13]Centre of Physical Activity and Nutrition (C-PAN) Research, School of Exercise and Nutrition Sciences, Deakin University, Burwood 3125, Australia
[14]Biomedical and Lifestyle Diseases (BioLED) Unit, School of Biomedical and Health Sciences, Victoria University, St Albans 3021, Australia
[15]Centre for Obesity Research and Education (CORE), Monash University, The Alfred Hospital, Melbourne 3004, Australia
[16]Department of Medicine, University of Virginia School of Medicine, Charlottesville, VA 22908, USA
[17]Department of Nutrition, Case Western University School of Medicine Cleveland, OH 44106, USA
*Correspondence: alarner@vcu.edu
http://dx.doi.org/10.1016/j.cmet.2012.11.005

SUMMARY

Mice lacking the Jak tyrosine kinase member Tyk2 become progressively obese due to aberrant development of Myf5+ brown adipose tissue (BAT). Tyk2 RNA levels in BAT and skeletal muscle, which shares a common progenitor with BAT, are dramatically decreased in mice placed on a high-fat diet and in obese humans. Expression of Tyk2 or the constitutively active form of the transcription factor Stat3 (CAStat3) restores differentiation in Tyk2$^{-/-}$ brown preadipocytes. Furthermore, Tyk2$^{-/-}$ mice expressing CAStat3 transgene in BAT also show improved BAT development, normal levels of insulin, and significantly lower body weights. Stat3 binds to PRDM16, a master regulator of BAT differentiation, and enhances the stability of PRDM16 protein. These results define Tyk2 and Stat3 as critical determinants of brown fat lineage and suggest that altered levels of Tyk2 are associated with obesity in both rodents and humans.

INTRODUCTION

Obesity occurs when caloric intake exceeds energy expenditure with excess nutrients stored as fat. There are two functionally different types of fat: white adipose tissue (WAT) and brown adipose tissue (BAT). WAT is the primary site of energy storage and also synthesizes and releases a variety of cytokines and hormones that modulate the actions of insulin. Obesity results from excessive accumulation of WAT. In contrast to WAT, BAT is responsible for energy expenditure in the form of thermogenesis. Uncoupling protein 1 (UCP1) is expressed only in BAT and uncouples oxidative phosphorylation from ATP generation, resulting in the production of heat instead of ATP. BAT deposits are present in all mammals, but in humans these deposits were believed to be nonfunctional except in newborns. However, over the past 4 years, it has become evident that BAT has an important role in human adults in the regulation of energy expenditure (Cypess et al., 2009; Nedergaard et al., 2007; Saito et al., 2009; Virtanen et al., 2009; Zingaretti et al., 2009). These studies indicate that BAT activity is inversely correlated with the severity of the metabolic syndrome and that BAT is a major contributor to maintain a lean phenotype. Thus, intervention to increase BAT activity and/or mass is a viable strategy to treat obesity.

Canonical activation of the Jak/Stat pathway involves cytokine and growth factors binding to their cell surface receptors, resulting in activation of one or several Jak kinases that tyrosine phosphorylate specific residues in the cytoplasmic domains of the receptors. Tyrosine phosphorylated receptors provide docking sites for the Stats through their SH2 domains. The activated Jaks also phosphorylate tyrosine on one or several Stats (Raz et al., 1994; Stark et al., 1998). Tyrosine phosphorylated Stats

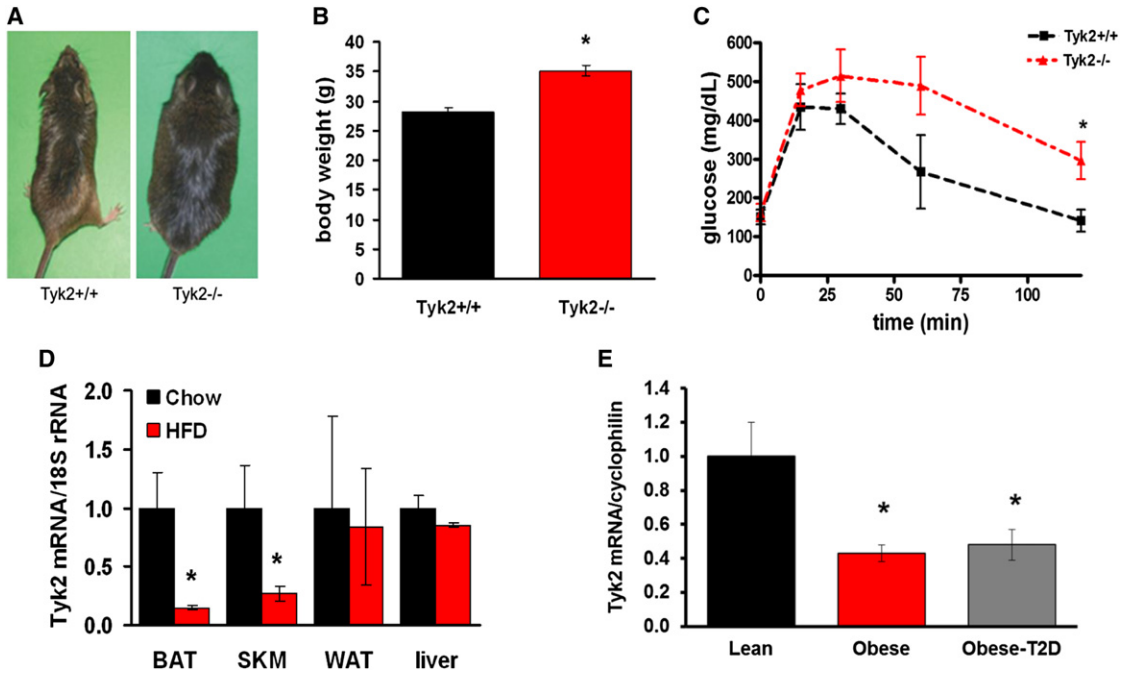

Figure 1. Tyk2$^{-/-}$ Mice Develop Metabolic Abnormalities

(A) Mice pictured at 12 months of age.

(B) Body weight of mice fed a normal chow diet at 16 weeks of age (n = 5–8 mice per group).

(C) Glucose tolerance test in Tyk2$^{+/+}$ and Tyk2$^{-/-}$ mice. Sixteen-week-old mice were fasted for 16 hr and injected intraperitoneally (IP) with 2 mg glucose/g body weight. Blood was collected from the tail vein and glucose was measured at the indicated times (n = 5–8 mice per group).

(D) Tyk2 RNA levels in BAT and skeletal muscle (SKM) are decreased in mice on a HFD. Five-week-old mice were placed on a normal chow or HFD for 12 weeks and RNA was harvested from BAT, SKM, WAT, and liver. RNAs corresponding to Tyk2, Jak1, and Jak2 were measured by qPCR (n = 5 mice per group).

(E) Tyk2 RNA levels are decreased in muscle samples from obese patients with or without T2D (n = 10–15 subjects per group).

Data are expressed as means ± SEM. See also Figures S1 and S2 and Table S1.

form homodimers or heterodimers, translocate to the nucleus, and bind to regulatory elements in the promoters of cytokine-stimulated early response genes (Decker et al., 1991; Pearse et al., 1991). Activation of the Jak kinase Tyk2 leads to tyrosine phosphorylation of Stat3 in response to different cytokines including type I interferons, IL-12 and IL-23.

No evidence has existed that Tyk2, a Jak kinase family member, has a role in the pathogenesis of obesity. In this study, we identify a role for Tyk2 in differentiation of Myf5+ brown adipocytes, and that Tyk2$^{-/-}$ mice become obese with age. Furthermore, Tyk2 levels are regulated by diet in mice, and Tyk2 levels are decreased in obese humans. Expression of constitutively active Stat3, (CAStat3) can restore BAT differentiation of Tyk2$^{-/-}$ preadipocytes and reverse the obese phenotype in Tyk2$^{-/-}$ mice. Moreover, rosiglitazone-induced stabilization of PRDM16 protein is absent in Stat3$^{-/-}$ brown preadipocytes under conditions, where there is no change in levels of PRDM16 RNA, suggesting another mechanism of Stat3 action. The data in this proposal provide evidence for the role of Tyk2 and Stat3 in the regulation of BAT differentiation and energy balance

RESULTS

Mice that Do Not Express Tyk2 Develop Obesity

We observed that Tyk2$^{-/-}$ mice weighed more than their wild-type littermates. By 12 months of age, the Tyk2$^{-/-}$ animals were approximately 20 g heavier than Tyk2$^{+/+}$ mice (Figure 1A). However, increased weights were observed as early as 12–16 weeks of age on normal chow diet (Figure 1B). Tyk2$^{-/-}$ mice displayed abnormal glucose clearance suggestive of insulin resistance (Figure 1C), as well as many other metabolic abnormalities, including elevated plasma insulin, cholesterol and free fatty acid levels (Table S1 available online). Due to different susceptibilities of many mice strains to developing obesity, we examined whether Tyk2$^{-/-}$ mice on C57BL/6 and SV129 backgrounds became obese. Both Tyk2$^{-/-}$ mice on a C57BL/6 and SV129 background showed augmented weights on a normal chow diet. Furthermore, we observed the same metabolic defects in B10.Q/J mice that have a spontaneous mutation in Tyk2 (data not shown) (Shaw et al., 2003). A complete metabolic profile was obtained on 12-week-old animals. When normalized to lean body mass (LBM) Tyk2$^{-/-}$ mice showed lower energy expenditure (Figures S1A and S1B) and produced 20% less heat (Figure S1C) during both day and night cycles. No changes in food intake (Tyk2$^{+/+}$, 13.4 ± 5.5 g/48 hr versus Tyk2$^{-/-}$, 12.9 ± 2.6 g/48 hr) or physical activity were detected between Tyk2$^{+/+}$ and Tyk2$^{-/-}$ mice.

Tyk2 Expression Is Reduced in Obese Mice and Humans

Tyk2 is a ubiquitously expressed protein, whose concentrations vary between tissues (Strobl et al., 2011). The protein is abundant in BAT, WAT and spleen and is present in lower

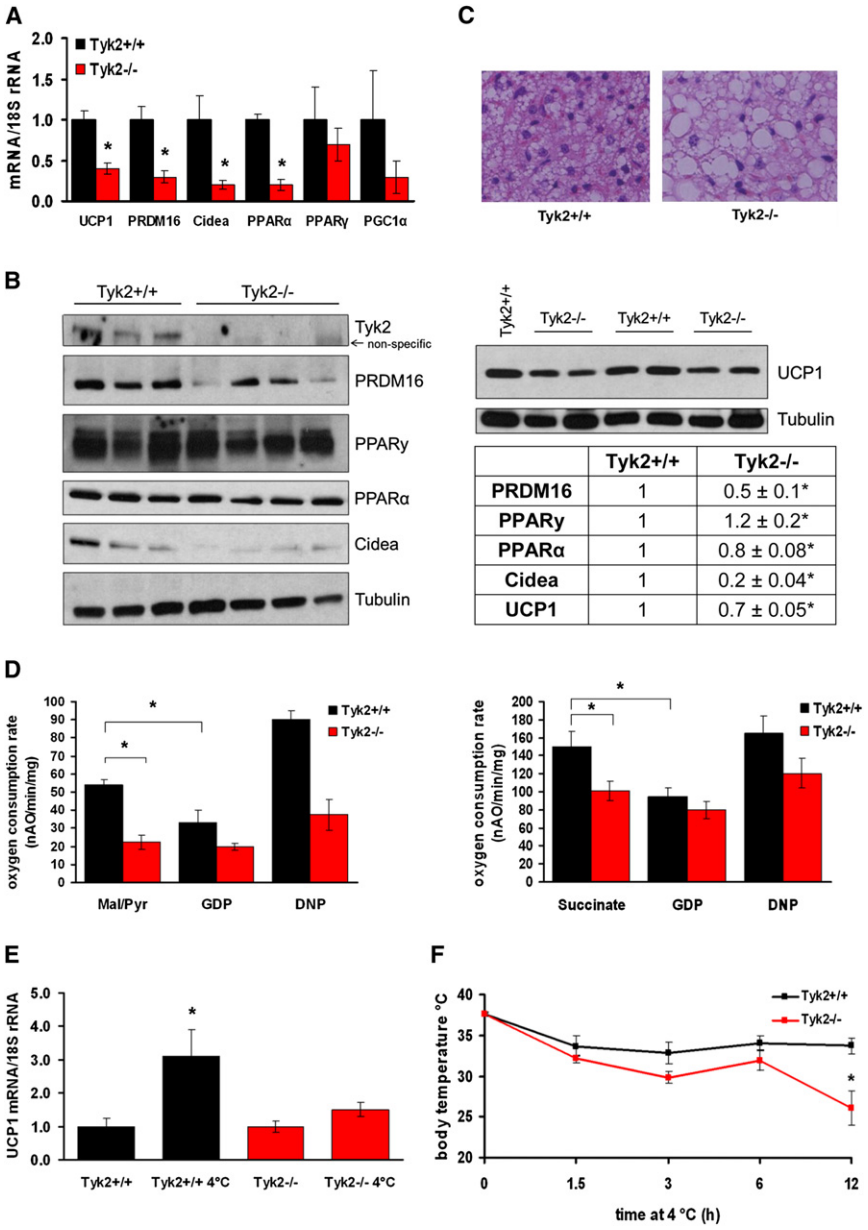

	Tyk2+/+	Tyk2-/-
PRDM16	1	0.5 ± 0.1*
PPARy	1	1.2 ± 0.2*
PPARα	1	0.8 ± 0.08*
Cidea	1	0.2 ± 0.04*
UCP1	1	0.7 ± 0.05*

Figure 2. Tyk2$^{-/-}$ Mice Display Impaired BAT Function

(A) BAT-specific RNAs (UCP1, PRDM16, and Cidea) are decreased in interscapular BAT isolated from 16-week-old Tyk2$^{-/-}$ mice. RNAs highly expressed in BAT (PPARγ and PGC1α) are not significantly changed in BAT isolated from Tyk2$^{-/-}$ mice (n = 5–8 mice per group).

(B) The amounts of BAT-selective proteins are decreased in Tyk2$^{-/-}$ mice. Cell extracts from BAT of individual Tyk2$^{+/+}$ and Tyk2$^{-/-}$ mice were analyzed by western blotting for the presence of PRDM16, PPARy, PPARα, Cidea, and UCP1 (n = 5–8 mice per group). Intensity of signals were quantified by Image J software and presented in the table. All samples were normalized to tubulin. The values represent mean fold decrease ± SE over Tyk2$^{+/+}$ set as 1.

(C) Hematoxylin and eosin staining of BAT from 16-week-old Tyk2$^{+/+}$ and Tyk2$^{-/-}$ mice (n = 4 mice per group).

(D) Oxygen consumption rates measured for isolated brown adipose tissue mitochondria are reduced in Tyk2$^{-/-}$ mice. Mitochondria were incubated under conditions described in the Experimental Procedures section. Data represent five separate experiments.

(E) UCP1 RNA in BAT is elevated in Tyk2$^{+/+}$ but not Tyk2$^{-/-}$ mice upon cold exposure. Mice were placed at 4°C for 12 hr prior to collection of RNA from BAT (n = 5 mice per group).

(F) Body temperatures measured with a rectal thermometer in Tyk2$^{+/+}$ and Tyk2$^{-/-}$ mice placed at 4°C (n = 5 mice per group).

Data are expressed as means ± SEM. See also Figures S3 and S4.

amounts in SKM and liver (Figure S2A). We examined whether changes in energy expenditure might control the levels of Tyk2 expression in tissues. C57BL/6 Tyk2$^{+/+}$ mice were placed on a high-fat diet (HFD) for 12 weeks, and Tyk2, Jak1, and Jak2 RNAs were analyzed in liver, skeletal muscle (SKM), BAT, and WAT. Tyk2 RNA was selectively decreased in BAT and skeletal muscles by approximately 70% in mice on a HFD compared to those on normal chow (Figure 1D), whereas Tyk2 RNA levels in WAT or liver were not changed. The expression of Tyk2 protein was also significantly decreased by 56% ($p < 0.05$) in BAT from mice placed on a HFD (Figure S2B). Levels of Tyk2 protein in SKM from animals on a HFD were decreased 50% ($p < 0.05$). Jak1 and Jak2 RNAs were not altered in mice placed on a HFD (Figures S2C and S2D). Similarly to mice fed a HFD, leptin-deficient mice (*ob/ob*) also displayed decrease in Tyk2, but not Jak1 or Jak2 RNA in BAT (Figure S2E).

We also examined the levels of Tyk2 RNA from rectus abdominus muscle samples obtained from obese humans with or without type II diabetes (T2D). Tyk2 RNA levels were 57% lower in the obese subjects and 52% lower in the obese-diabetic subjects, when compared with lean control subjects (Figure 1E). There were no differences in Jak1 or Jak2 expression between the groups (Figure S2F).

Tyk2$^{-/-}$ Mice Show Abnormal BAT Development

Reduced energy expenditure in Tyk2$^{-/-}$ mice suggested additional abnormalities in BAT-specific gene expression in Tyk2$^{-/-}$ mice. Expression of UCP1, PRDM16, and Cidea (cell death-inducing DFFA-like effector a) was diminished in BAT isolated from 16-week-old Tyk2$^{-/-}$ mice compared with wild-type animals (Figure 2A). Additionally, Tyk2$^{-/-}$ mice showed a defect in the expression of β oxidation enzymes AOX (acyl-CoA oxidase) and LCAD (long chain acyl-CoA dehydrogenase) in BAT (Figure S1D). However, RNAs that are normally highly expressed in BAT like PPARγ and PGC1α were not different between Tyk2$^{+/+}$ and Tyk2$^{-/-}$ animals. The protein levels corresponding to these

Table 1. Reduced Gene Expression in Tyk2-Deficient Adipocytes Is Restored by Reconstitution with CAStat3 and Partially with Tyk2

	$Tyk2^{+/+}$	$Tyk2^{-/-}$	$Tyk2^{-/-}$ + MSCV	$Tyk2^{-/-}$ + Tyk2	$Tyk2^{-/-}$ + CAStat3
UCP1	1	0.1 ± 0.03*	0.1 ± 0.04*	0.5 ± 0.1	1.3 ± 0.4
PRDM16	1	0.1 ± 0.04*	0.2 ± 0.07*	0.3 ± 0.09*	1.1 ± 0.4
Cidea	1	0.2 ± 0.07*	0.2 ± 0.07*	0.4 ± 0.2*	2.3 ± 0.6
Elovl3	1	0.3 ± 0.17*	0.5 ± 0.2*	0.6 ± 0.4*	1.5 ± 0.5
PGC1α	1	0.1 ± 0.02*	0.1 ± 0.02*	0.2 ± 0.09*	1.7 ± 0.7
PPARα	1	0.3 ± 0.1*	0.3 ± 0.04*	0.2 ± 0.08*	1.2 ± 0.6
PPARγ	1	0.2 ± 0.05*	0.2 ± 0.06*	0.3 ± 0.07*	1.8 ± 0.4
MCK	1	8.4 ± 2.0*	6.3 ± 1.4*	2.7 ± 0.5	3.4 ± 0.5*
MyoD	1	7.5 ± 1.7*	10 ± 2.2*	2.9 ± 0.5	4.3 ± 0.7*
Myg	1	12 ± 2.1*	29 ± 1.3*	2.6 ± 0.2	3.5 ± 1.7*

Total RNA was isolated from in vitro differentiated adipocytes and analyzed for selected RNA levels using qPCR. The values represent mean fold change ± SEM over $Tyk2^{+/+}$ set as 1, for n = 5 independent experiments. See also Figure S4.

RNAs were also decreased in BAT of $Tyk2^{-/-}$ mice (Figure 2B). Defects in the morphology of BAT from $Tyk2^{-/-}$ animals were obvious by hematoxylin and eosin staining. $Tyk2^{-/-}$ BAT cells contained large unilocular fat droplets, whereas $Tyk2^{+/+}$ BAT showed multilocular fat droplets (Figure 2C).

We also examined the mitochondrial morphology of BAT from $Tyk2^{+/+}$ and $Tyk2^{-/-}$ mice using transmission electron microscopy. The mitochondria of $Tyk2^{-/-}$ BAT and skeletal muscle showed disorganized cristae, but no alterations in mitochondria morphology was observed in the heart (Figure S3A).

Mitochondrial function and ultrastructure depend on the proper fusion of the outer and inner membranes (Zick et al., 2009). The fusion processes are governed by three large GTPases: mitofusin 1 (Mfn1), mitofusin 2 (Mfn2), and optic atrophy protein 1 (OPA1). Mfn1 and Mfn2 are involved in early steps of outer membrane fusion, whereas OPA1 is associated with inner membrane fusion and cristae remodeling (Chen and Chan, 2010). Disorganization of mitochondrial cristae observed in BAT and skeletal muscles from Tyk2-deficient mice correlated with decreased OPA1 expression in these tissues (Figure S3B). Reduced mRNA levels of OPA1 were not observed in the control tissues, such as WAT or liver. The expression levels of Mfn1 in SKM and Mfn2 in BAT were modestly changed (Figures S3C and S3D). It is notable that elevated expression of these RNAs is associated with an insulin-sensitive phenotype in humans (Lidell et al., 2011). Since BAT and skeletal muscles originate from the same Myf5-positive progenitor cells (Seale et al., 2008), we conclude that Tyk2 kinase may be important at an early stage of development of these progenitors.

To further confirm a functional defect in $Tyk2^{-/-}$ BAT, we performed oxygen consumption assays using isolated mitochondria from $Tyk2^{+/+}$ or $Tyk2^{-/-}$ BAT (Figure 2D). Compared with $Tyk2^{+/+}$ mitochondria, oxygen consumption was decreased in $Tyk2^{-/-}$ mitochondria when pyruvate and malate were used as substrates for complex I activity and succinate for complex II activity. Addition of GDP, which inhibits the activity of UCP1, decreased O_2 consumption of $Tyk2^{+/+}$, but not $Tyk2^{-/-}$, mitochondria. The addition of DNP (an uncoupler of OXPHOS) increased O_2 consumption of $Tyk2^{+/+}$ and $Tyk2^{-/-}$ mitochondria. The respiratory activities of $Tyk2^{-/-}$ mitochondria were comparable to those reported in BAT mitochondria from UCP1-deficient mice (Dlasková et al., 2010).

Since BAT plays a central role in nonshivering thermogenesis, which maintains body temperature during cold exposure, we examined body temperature and the induction of UCP1 in mice exposed to 4°C for 12 hr. There was a significant induction in UCP1 RNA in BAT in $Tyk2^{+/+}$ but not in $Tyk2^{-/-}$ mice (Figure 2E). Body temperatures were also significantly lower in $Tyk2^{-/-}$ animals (Figure 2F). The mechanisms for enhanced sensitivity to cold in $Tyk2^{-/-}$ mice may be due to dysfunctional BAT, which controls nonshivering thermogenesis and/or from a defect in skeletal muscle that is responsible for shivering thermogenesis.

Constitutively Active Stat3 and PRDM16 Restore Differentiation of $Tyk2^{-/-}$ Brown Adipocytes

Decrease in BAT-specific RNAs was also observed in in vitro differentiated brown preadipocytes isolated from the interscapular BAT of $Tyk2^{-/-}$ mice (Table 1). $Tyk2^{-/-}$ preadipocytes did not differentiate as indicated with oil red O staining (Figure 3A). $Tyk2^{-/-}$ preadipocytes were infected with retroviruses expressing Tyk2, constitutively active Stat3 (CAStat3) or the empty vector (MSCV) and subjected to in vitro differentiation (Tseng et al., 2004). Cells expressing Tyk2 or CAStat3, but not the control vector, became oil red O positive (Figure 3A). Levels of BAT-specific RNAs were completely restored by expression of CAStat3 and were partially restored by Tyk2 (Table 1). The explanation as to why the expression of wild-type Tyk2 failed to completely restore BAT-specific RNAs is not clear.

Since BAT and skeletal muscle share a common progenitor, and PRDM16 levels are diminished in $Tyk2^{-/-}$ preadipocytes (Seale et al., 2008), we analyzed expression of skeletal muscle-specific genes. The three muscle-selective markers MCK, MyoD, and Myg were all elevated in $Tyk2^{-/-}$ compared with $Tyk2^{+/+}$ preadipocytes (Table 1, lower portion). Interestingly, the expression of CAStat3 in $Tyk2^{-/-}$ preadipocytes was much less effective than Tyk2 in decreasing the levels of muscle-specific RNAs (Table 1). These results suggest that there are two different functions of Tyk2: One is to induce the expression of BAT-specific genes, which is effectively accomplished by the expression of Tyk2 or CAStat3. The other is the repression of skeletal muscle markers, which requires Tyk2 and is poorly restored by the expression of CAStat3.

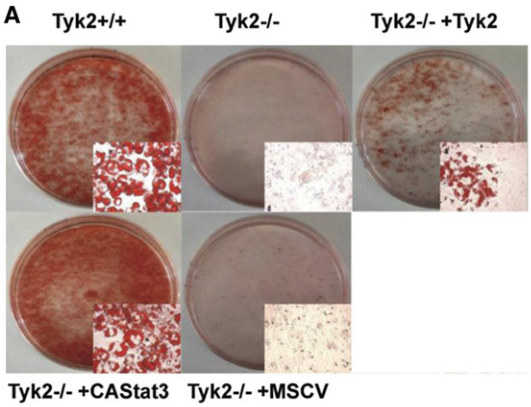

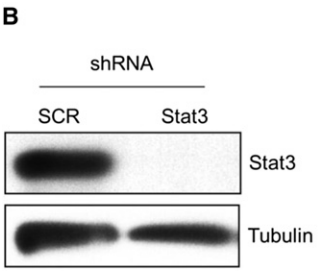

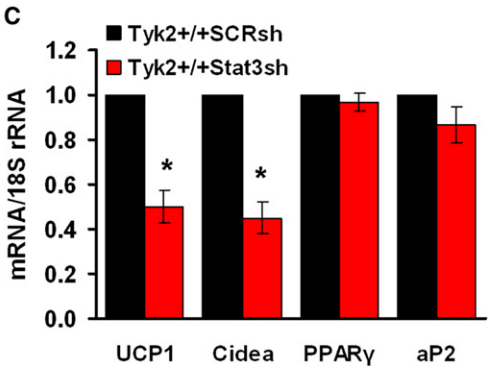

Figure 3. Expression of Tyk2 and Stat3 Are Required for Differentiation of Brown Adipocytes

(A) Expression of Tyk2 or CAStat3 in immortalized Tyk2$^{-/-}$ preadipocytes restores lipid accumulation. Cell lines were subjected to in vitro differentiation and stained with working solution of oil red O.

(B) Stat3 protein level in Tyk2$^{+/+}$ preadipocytes infected with shRNA directed against Stat3 or a scrambled control (SCR).

(C) Amount of brown adipose tissue-specific (UCP1, Cidea) and adipogenic (PPARγ, aP2) RNAs in Stat3 shRNA- or SCR control shRNA-expressing adipocytes (n = 4 independent experiments). Data are expressed as means ± SEM.

UCP1 and Cidea are expressed in BAT and their expression in brown adipocytes is regulated by DNA methylation and chromatin remodeling (Karamanlidis et al., 2007; Karamitri et al., 2009; Shore et al., 2010). Using bisulphite sequencing, we determined the methylation status of the CpGs in the promoters of UCP1 and Cidea genes. We observed hypermethylation of DNA within these promoters in Tyk2$^{-/-}$ preadipocytes (Figure S4A), especially at the regions containing the C/EBPβ binding sites, which are crucial for the expression of UCP1 and Cidea (red frames in Figure S4A). Furthermore, the abundance of trimethylated histone H3 at lysine 4 (H3K4me3), which is a mark of transcriptionally active chromatin, was lower in the UCP1 and Cidea promoters in Tyk2$^{-/-}$ differentiated brown adipocytes (Figures S4B and S4C). As an internal control, we examined the abundance of H3K4me3 at the p16 promoter, which was the same in Tyk2$^{+/+}$ and Tyk2$^{-/-}$ preadipocytes (Figure S4D). p16 expression and methylation are not affected by BAT differentiation.

Since CAStat3 rescues differentiation in Tyk2$^{-/-}$ preadipocytes, we examined whether Stat3 was required for brown adipocyte differentiation. Stable preadipocyte lines were created using short hairpin RNA (shRNA) directed against Stat3 or a scrambled control (SCR). Western blot analysis showed complete loss of Stat3 protein (Figure 3B), which correlated with decreases in BAT-specific gene expression (UCP1, Cidea) but not in adipogenic markers (PPARγ and aP2) (Figure 3C). The normal levels of PPARγ and aP2 in these cells is consistent with the observation that they display normal adipogenesis and become oil red O positive (data not shown).

PRDM16 and C/EBPβ control the conversion of myoblastic precursors to brown adipocytes and are sufficient to induce differentiation of fully functional brown adipocytes from nonadipogenic embryonic fibroblasts (Seale et al., 2008; Seale et al., 2007). Since PRDM16 is a master regulator of BAT development, we tested whether its overexpression could induce differentiation in Tyk2$^{-/-}$ preadipocytes. Tyk2$^{-/-}$ cells were infected with retroviruses expressing PRDM16 and/or C/EBPβ. PRDM16 expression increased the differentiation of brown adipocytes as demonstrated both by oil red O staining (Figure 4A) and gene expression (Table 2). Expression of C/EBPβ alone had no effect on differentiation of Tyk2$^{-/-}$ brown preadipocytes (Figure 4A). However, a combination of both PRDM16 and C/EBPβ fully restored differentiation of Tyk2$^{-/-}$ preadipocytes to the level observed in Tyk2$^{+/+}$ cells. Furthermore, immunoprecipitation of PRDM16 from these cells demonstrated that endogenous Stat3 formed a complex with PRDM16 (Figure 4B). We have also detected the complex in cell extracts immunoprecipitated with Stat3 (Figure 4C), as well as in adipocytes, which express endogenous levels of PRDM16 and Stat3 (Figure 4D). We have not observed any changes in the association of PRDM16 and Stat3 in cells treated with rosiglitazone (data not shown).

Stat3 Enhances Stability of PRDM16

Treatment of preadipocytes with the PPARγ agonist rosiglitazone stabilizes PRDM16 protein (Ohno et al., 2012). Since PRDM16 interacts with Stat3 and the expression of both is required for differentiation of brown adipocytes, we examined PRDM16 protein levels in Stat3$^{+/+}$ and Stat3$^{-/-}$ preadipocytes incubated with or without rosiglitazone, while the cells were being differentiated (Figure 4E). Basal levels of PRDM16 protein were very much decreased or absent in differentiated Stat3$^{-/-}$ adipocytes, and rosiglitazone induction of PRDM16 was severely blunted. We also incubated cells with or without rosiglitazone under nondifferentiating conditions (Figure 4F). Although basal levels of PRDM16 were similar in Stat3$^{+/+}$ and Stat3$^{-/-}$ cells prior to differentiation, rosiglitazone did not increase the

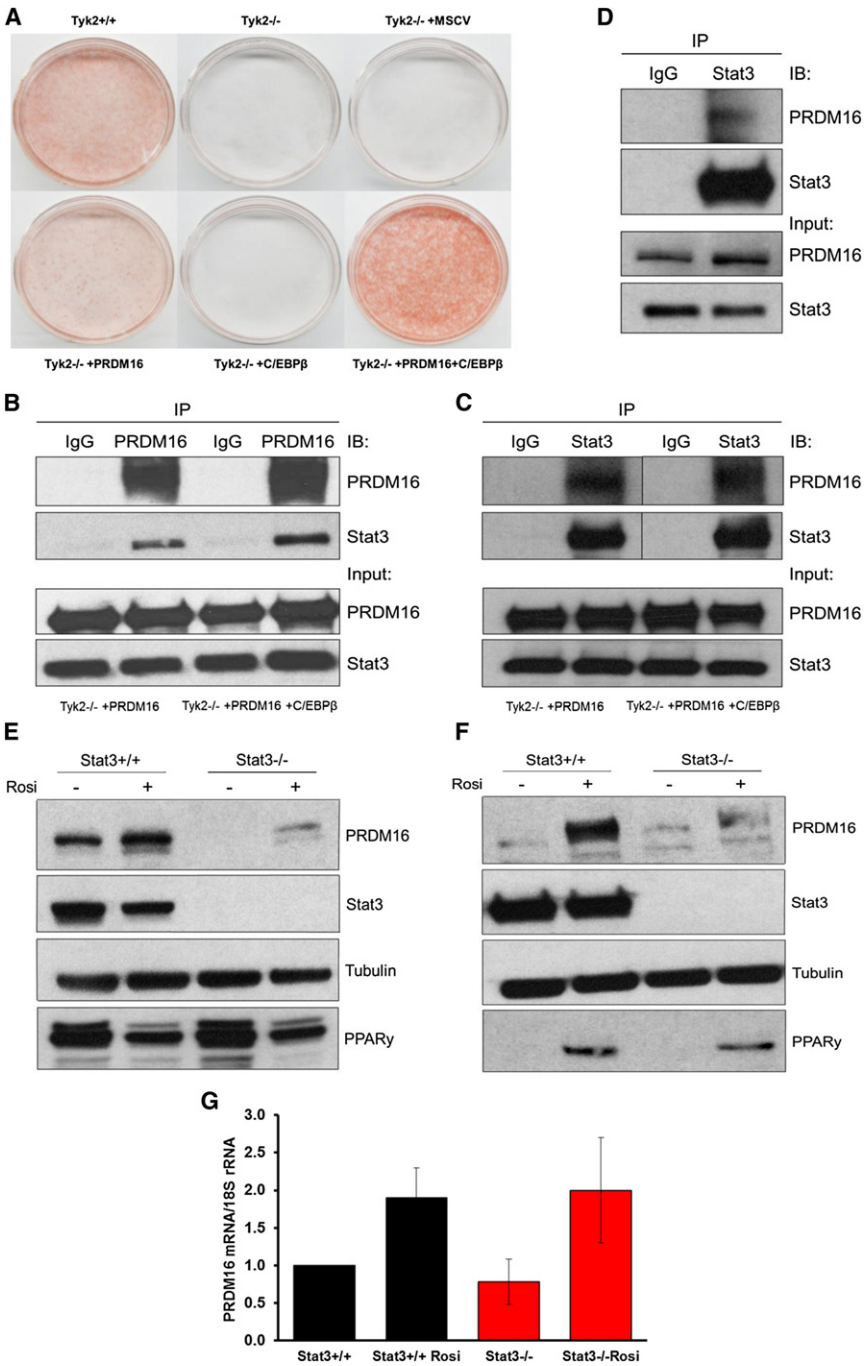

Figure 4. PRDM16 and Stat3 Regulate Differentiation of Brown Preadipocytes

(A) Oil red O staining of immortalized brown adipocytes expressing indicated retroviral vectors 5 days after inducing adipocyte differentiation (n = 3 independent experiments).

(B) Stat3 coimmunoprecipitates with PRDM16. Cell extracts prepared from differentiated Tyk2$^{-/-}$ adipocytes expressing PRDM16 or PRDM16 and C/EBPβ were immunoprecipitated with either IgG (lanes 1 and 3) or PRDM16 (lanes 2 and 4) antisera. The immunoblots were probed for either PRDM16 or Stat3. Endogenous Stat3 was detected in the complex with PRDM16 by western blotting. Input is shown in the lower panels. IB, immunoblot; IP, immunoprecipitate (n = 3 independent experiments).

(C) The same cell extracts used in (B) were immunoprecipitated with either IgG or Stat3 antisera. The immunoblots were probed for either PRDM16 or Stat3. Input is shown in the lower panels (n = 3 independent experiments).

(D) Cell extracts from differentiated wild-type brown adipocytes were immunoprecipitated with either IgG or Stat3 antisera. The immunoblots were probed for either PRDM16 or Stat3. Input is shown in the lower panels (n = 2 independent experiments).

(E) Stat3$^{-/-}$ adipocytes are insensitive to rosiglitazone-induced accumulation of PRDM16. Cell lines were generated from immortalized Floxed Stat3$^{+/+}$ preadipocytes infected with a retrovirus expressing Cre recombinase or an empty vector control. Cell lines were differentiated in the presence or absence of rosiglitazone (1 μM). Extracts were western blotted for the expression of PRDM16, Stat3, and tubulin as a control for protein loading (n = 4 independent experiments).

(F) The same Stat3$^{+/+}$ and Stat3$^{-/-}$ cell lines were incubated with or without rosiglitazone (1 μM) for 4 days (nondifferentiating conditions). Protein extracts western blotted for the expression of PRDM16, Stat3, and tubulin as a control for protein loading (n = 3 independent experiments).

(G) Stat3 expression does not affect cellular levels of PRDM16 RNA. Cells were exposed to rosiglitazone as described in C). RNA was harvested and PRDM16 transcripts were measured by qPCR (n = 4 independent experiments). Data are expressed as means ± SEM.

expression of PRDM16 in Stat3$^{-/-}$ cells. Furthermore, expression of PPARγ was not altered in Stat3$^{-/-}$ preadipocytes.

In contrast to levels of PRDM16 protein, as reported by Ohno et al. (2012), levels of PRDM16 RNA were not significantly changed in Stat3$^{+/+}$ or Stat3$^{-/-}$ brown adipocytes with or without exposure to rosiglitazone (Figure 4G).

Expression of Constitutively Active Stat3 in BAT Protects Tyk2$^{-/-}$ Mice from Becoming Obese

To determine whether the metabolic syndrome in Tyk2$^{-/-}$ mice was due to a defect in BAT development, we examined a mouse containing a constitutively active Stat3 transgene, whose expression is activated by Cre recombinase (Mesaros et al., 2008). CAStat3 mice were crossed with Tyk2$^{-/-}$ mice (Tyk2$^{-/-}$CAStat3). Tyk2$^{-/-}$CAStat3 mice were then crossed with aP2 Cre/Tyk2$^{-/-}$ mice that express Cre recombinase in adipose tissue to generate aP2-Cre/Tyk2$^{-/-}$CAStat3 mice (Imai et al., 2001). Consistent with the results of Mesaros et al. (2008), the transgene was expressed at physiological levels (data not shown). All experiments were performed using Tyk2$^{-/-}$ CAStat3 (controls; CTR) and animals with the activated transgene aP2-Cre/Tyk2$^{-/-}$CAStat3 (CAStat3), from the same litter.

Table 2. Reconstitution of Brown Adipose Tissue-Specific Gene Expression in Tyk2$^{-/-}$ Preadipocytes through PRDM16 and C/EBPβ

	Tyk2$^{+/+}$	Tyk2$^{-/-}$	Tyk2$^{-/-}$ + MSCV	Tyk2$^{-/-}$ + PRDM16	Tyk2$^{-/-}$ + C/EBPβ	Tyk2$^{-/-}$ + PRDM16 + C/EBPβ
UCP1	1	0.2 ± 0.09*	0.2 ± 0.1*	1.4 ± 0.35	0.1 ± 0.7*	1.1 ± 0.08
PRDM16	1	0.2 ± 0.07*	0.3 ± 0.1*	760 ± 84	0.2 ± 0.03*	1150 ± 307
Cidea	1	0.1 ± 0.03*	0.1 ± 0.03*	0.45 ± 0.1*	0.1 ± 0.04*	2.9 ± 0.3
Elovl3	1	0.2 ± 0.09*	0.2 ± 0.1*	0.2 ± 0.05*	0.3 ± 0.1*	2.1 ± 0.6
PGC1α	1	0.1 ± 0.02*	0.1 ± 0.03*	0.5 ± 0.15*	0.2 ± 0.06*	2.7 ± 0.8
PPARα	1	0.3 ± 0.2*	0.3 ± 0.2*	0.95 ± 0.15	0.4 ± 0.2*	1.0 ± 0.1
PPARγ	1	0.2 ± 0.09*	0.2 ± 0.04*	0.4 ± 0.1*	0.3 ± 0.1*	1.2 ± 0.4

Total RNA was isolated from in vitro differentiated adipocytes and analyzed for selected RNA levels. The values represent mean fold change ± SEM over Tyk2$^{+/+}$ set as 1, for n = 4 independent experiments.

As previously reported, transgenes expressed under the control of the aP2 promoter can be variably expressed in BAT, WAT, or both tissues (Cho et al., 2009). Expression of the CAStat3 transgene preferentially in BAT of Tyk2$^{-/-}$ mice upregulated the levels of BAT-specific RNAs (UCP1, PRDM16, Cidea), which are severely diminished in Tyk2$^{-/-}$ animals (Figure 5A). C/EBPβ, PPARγ, and PPARα, which play important roles in BAT development, were also increased. The protein levels corresponding to these RNAs were also increased in BAT of CAStat3 mice (Figure 5B). Furthermore, the altered BAT morphology depicted in (Figure 2C) was restored by CAStat3 expression and resembled the tissue in wild-type animals (Figure 5C). Tyk2$^{-/-}$ mice expressing CAStat3 in BAT exhibited significantly reduced body weight in comparison to control littermates (Figure 5D). Moreover, CAStat3 mice had much lower plasma insulin levels than control animals, suggesting improved insulin sensitivity (Figure 5E). The levels of insulin as well as body weight in the transgeneic mice were similar to wild-type animals (data not shown).

DISCUSSION

The data in this report provide evidence for the unanticipated role of Tyk2 and Stat3 in the regulation of Myf5+ BAT development and energy balance both in rodents and possibly humans. Tyk2$^{-/-}$ mice provide a model to understand the role of BAT in pathogenesis of obesity. The observations that Tyk2 RNA in BAT and skeletal muscle is regulated by diet in rodents, and obese humans, who also have decreased levels of Tyk2 in skeletal muscle, offers potential avenues for pharmacological and nutritional intervention to treat obesity.

At the moment it is not clear whether the obese phenotype observed in Tyk2$^{-/-}$ mice is only due to impaired differentiation of BAT or whether a defect in SKM also contributes to obesity. Since we have used global Tyk2 knock out animals for these studies, it is also possible that the changes in overall metabolism are a result of a multiple defects in more than one tissue. The fact that the CAStat3 transgene expressed in BAT of Tyk2$^{-/-}$ mice restores a normal phenotype argues that the actions of Stat3 do not required its activation in SKM. These results also argue against the concept that a defect in many tissues in the Tyk2$^{-/-}$ mouse is required for the development of obesity. It remains to be determined whether the actions of Tyk2 are mediated through Stat3 and/or another signaling pathway.

White and brown adipocytes are derived from mesenchymal stem cells. Interscapular BAT shares a common lineage with Myf5+ muscle progenitors, while brown adipocyte-like cells distributed within subcutaneous WAT and skeletal muscle have a different lineage (Schulz et al., 2011). Recent studies indicate that this model is more complex in that mixtures of Myf5+ and Myf5– cells are present in WAT (Sanchez-Gurmaches et al., 2012). Differentiation of Myf5+ progenitors into brown preadipocytes requires the expression of PRDM16. Our results suggest that Tyk2 and Stat3 are required for the progression of differentiation-incompetent preadipocytes to committed differentiation-competent brown preadipocytes such that PRDM16, C/EBPβ, Stat3, and other transcription factors can induce differentiation. It remains to be determined, whether Tyk2 and Stat3 directly or indirectly mediate the expression of BAT-selective RNAs. The fact that the DNA in the promoters of UCP1 and Cidea are hypermethylated in Tyk2$^{-/-}$ preadipocytes, and markers of the abundance of trimethylated histone H3 at lysine 4 (H3K4me3) are decreased is consistent with an effect of Tyk2 on chromatin modeling.

This leads us to speculate that the role of Tyk2 in differentiation of BAT is to directly or indirectly facilitate chromatin remodeling and accessibility. A nuclear-localized pool of the related kinase Jak2 phosphorylates histone H3 (Dawson et al., 2009). It is notable that Tyk2 also localizes to the nucleus (Ragimbeau et al., 2001). It is thus possible that the actions of Tyk2 are unrelated to those of Stat3 and classic cytokine activation of the Jak/Stat pathway. An alternative or additional role of Tyk2 might be to modify Stat3 such that in combination with PRDM16 and C/EBPβ it induces the expression of BAT-specific genes. Under this scenario, CAStat3 would be modified in the absence of Tyk2 such that it can induce differentiation of Tyk2$^{-/-}$ preadipocytes. Tyrosine phosphorylation of Stat3 probably is not the modification of this protein mediated by Tyk2 because both basal levels of tyrosine phosphorylated Stat3 in preadipocytes, and tyrosine phosphorylated Stat3 during differentiation are not different between Tyk2$^{-/-}$ and Tyk2$^{+/+}$ cells (data not shown). Acetylation and methylation have been reported to modify Stat3 and contribute to the effects of Stat3 in gluconeogenesis (Nie et al., 2009; Yang et al., 2010).

In contrast to the ability of CAStat3 to induce BAT-specific gene expression, CAStat3 does not substitute for wild-type Tyk2 in repressing the expression of muscle specific genes during differentiation of preadipocytes (Table 1). Disrupted expression of Stat3 in Tyk2$^{+/+}$ preadipocytes diminished BAT-selective gene expression, indicates that this transcription factor plays an essential role in two stages of BAT development: the

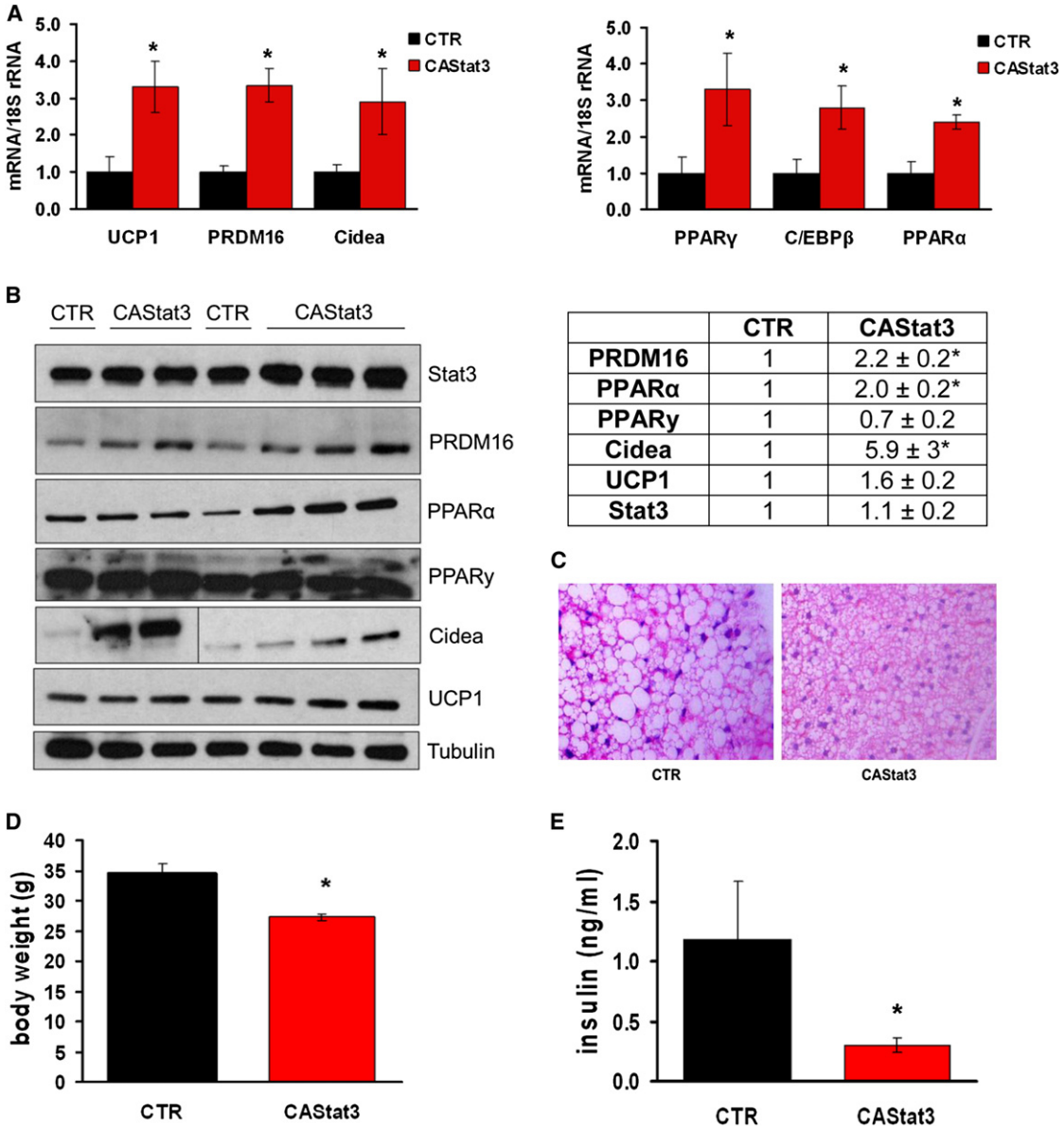

	CTR	CAStat3
PRDM16	1	2.2 ± 0.2*
PPARα	1	2.0 ± 0.2*
PPARγ	1	0.7 ± 0.2
Cidea	1	5.9 ± 3*
UCP1	1	1.6 ± 0.2
Stat3	1	1.1 ± 0.2

Figure 5. Expression of CAStat3 in BAT Reverses Obesity in Tyk2$^{-/-}$ Mice

(A) The BAT-specific RNA levels (UCP1, PRDM16, Cidea) and highly expressed BAT RNA expression (PPARγ, C/EBPβ, PPARα) are restored in tissue from Tyk2$^{-/-}$ mice that express the CAStat3 transgene. Total RNA was isolated from interscapular BAT of 12 week old mice (n = 6–8 mice per group).

(B) The amounts of BAT-enriched proteins are increased in CAStat3 mice. Cell extracts from BAT of individual control (CTR) and CAStat3 mice were analyzed by western blotting for the presence of PRDM16, PPARα, PPARγ, Cidea, and UCP1 (n = 6–8 mice per group). Intensity of signals were quantified by Image J software and presented in the table. All samples were normalized to tubulin. The values represent mean fold increase ± SE over CTR mice set as 1.

(C) Hematoxylin and eosin staining staining of interscapular BAT from 12-week-old CTR and CAStat3-expressing mice (n = 5 mice per group).

(D) Body weight of 24-week-old CAStat3 and control mice fed a regular chow diet (n = 10–12 mice per group).

(E) Fasted plasma insulin levels of 24-week-old control and CAStat3-expressing mice (n = 10–12 mice per group).

Data are expressed as means ± SEM.

progression of differentiation-incompetent to differentiation-competent preadipocytes and the development of differentiation-competent adipocytes into mature brown adipocytes. At the moment it is not clear whether progression from differentiation-competent to mature brown adipocytes requires Tyk2.

The expression of CAStat3 in BAT of Tyk2$^{-/-}$ mice is consistent with the results in cell culture models. However, the aP2 Cre promoter used to express CAStat3 in Tyk2$^{-/-}$ mice is also expressed in macrophages and brain, leaving the possibility that these tissues may also be involved in the obese phenotype (Klöting et al., 2008; Mao et al., 1993; Urs et al., 2006). We have not detected expression of CAStat3 in macrophages indicating that they do not contribute to the actions of CAStat3 in preventing the development of obesity. We have not examined, whether

CAStat3 mice express the transgene in brain. However, if CAStat3 expression in the brain is contributing to the prevention of obesity, then we would expect to see changes in the metabolic profile of mice that express CAStat3 only in WAT and brain. The limited numbers of animals that express CAStat3 only in WAT that have been examined, display the same phenotype as Tyk2$^{-/-}$ mice. These results suggest that it is unlikely that expression of CAStat3 in the brain is contributing to the obesity observed in Tyk2$^{-/-}$ mice.

The observation that rosiglitazone-induced stabilization of PRDM16 protein is absent in Stat3$^{-/-}$ brown preadipocytes under conditions, where there is no change in levels of PRDM16 RNA suggests another mechanism of Stat3 action. We have examined whether the expression of Stat3 controls the rate of degradation of PRDM16 by treating cells with cycloheximide (Ohno et al., 2012). There were no changes in half life of PRDM16 protein in Stat3$^{-/-}$ compared to Stat3$^{+/+}$ preadipocytes, suggesting that in these cells the rate of translation of PRDM16 is being influenced by the presence of Stat3. However, these results are ambiguous because the endogenous levels of PRDM16 are very low in Stat3$^{-/-}$ cells, which makes it very difficult to analyze rates of decay of the protein. Stat3 may directly stabilize PRDM16 protein, presumably by their direct interaction (Figures 4B–4D). Alternatively, Stat3 may regulate the expression of RNAs that encode proteins involved in stability of PRDM16. Since PRDM16 is destabilized through the ubiquitin (Ub)-proteasome targeting system, this complex is also a potential target of Stat3. In renal cancer cells Stat3 has been reported to bind and stabilize HIF1a but the physiological consequences of this interaction need to be clarified (Jung et al., 2005).

Further characterization of the mechanisms by which Tyk2 and Stat3 regulate brown fat development in animal models and a better understanding of the signaling cascade governed by these proteins will help design screens for different targets to treat obesity and the metabolic syndrome.

EXPERIMENTAL PROCEDURES

Subjects

Ten lean controls (four men, six women; average age, 45.3 ± 2.8), 15 obese (three men, 12 women; average age, 36 ± 2.1) and 12 obese type 2 diabetic (eight men, four women; average age, 49.3 ± 1.4) individuals participated in this study. Obese and obese type 2 diabetic patients were undergoing laparoscopically performed adjustable gastric banding surgery, as previously described (O'Brien et al., 2005). None of the patients were under thiazolidinedione but some of them under insulin treatment. Lean patients were undergoing general abdominal surgical procedures unrelated to obesity or type 2 diabetes. The subject details have been published previously (Russell et al., 2012). Written informed consent was obtained from all subjects. This study was approved by the Deakin University Human Ethics Research Committee, The Avenue Hospital and Cabrini Hospital. Muscle samples (about 200 mg) were obtained from the rectus abdominus in the fasted state (8–18 hr). All participants were under general anesthesia, predominantly via short-acting propofol and maintained by a fentanyl, rocuronium and volatile anesthesia mixture. Following collection, which was performed 30 min after the operation had started, surgical samples were immediately frozen in liquid nitrogen.

Statistical analysis was performed using SPSS version 15.0. A one-way analysis of variance (ANOVA) followed by LSD or Dunnett's T3 post hoc test was used (where equal variances were not assumed) to determine the significance of differences between groups. Significance was set at $p < 0.05$.

Animals

All the mice were bred and maintained in the MCV/VCU animal facility according to Institutional Animal Care and Use Committee (IACUC) regulations. Male mice were used for these studies. Tyk2-deficient mice (C57BL/6) were kindly provided by Dr. Ana Gamero (Temple University School of Medicine, Philadelphia, USA). Tyk2$^{-/-}$ (SV129) were generated by Dr. Kazuya Shimoda and colleagues (Kyushu University, Fukuoka, Japan) (Shimoda et al., 2000). Mice carrying a transgene encoding a constitutively active form of the Stat3 protein (CAStat3) including an upstream loxP- flanked stop sequence in the ubiquitously expressed Rosa26 locus were a kind gift of Dr. Klaus Rajewsky (Harvard Medical School, Boston, MA) (Mesaros et al., 2008). The Tyk2$^{-/-}$ mice expressing the constitutively active Stat3 only in BAT (brown adipose tissue) or WAT (white adipose tissue) were obtained by crossing CAStat3 transgenic animals with mice expressing the Cre recombinase under control of the aP2 promoter, allowing adipocyte-specific expression of Cre. Both transgenic lines (CAStat3 and aP2-Cre) were bred with Tyk2$^{-/-}$ mice and then intercrossed. Only animals from the same mixed background strain generation were compared. The specificity of transgene expression was confirmed by quantitative PCR (qPCR). Mice carrying floxed alleles of Stat3 were kindly provided by Dr. Valeria Poli (University of Turin, Turin, Italy).

Cell Culture

Interscapular brown adipose tissue was isolated from newborn Tyk2$^{+/+}$ and Tyk2$^{-/-}$ mice, minced and subjected to collagenase A digestion (1.5 mg/ml in isolation buffer containing 123 mM NaCl, 5 mM KCl, 1.3 mM $CaCl_2$, 5 mM glucose, 100 mM HEPES, and 4% BSA) for 40 min at 37°C (Fasshauer et al., 2000). Collected cells were centrifuged at 1,500 rpm at room temperature for 5 min and then resuspended in 1 ml primary culture medium (Dulbecco's modified Eagle medium, 4,500 mg/liter glucose GIBCO, Carlsbad, CA) containing 20% FBS, 20 mM HEPES, and 1% penicillin-streptomycin), transferred into 12-well plates and grown in a humidified atmosphere of 5% CO_2 and 95% O_2 at 37°C. After 3 days of culture, cells were immortalized by infection with puromycin resistance retroviral vector pBabe encoding SV40 Large T antigen. Twenty-four hours after infection cells were split into 10 cm dishes and maintained in primary culture media for the next 24 hr and then subjected to selection with puromycin at a concentration of 2 μg/ml in DMEM with 20% FBS for one week.

For differentiation, brown preadipocytes were grown to 100% confluence in the differentiation medium: DMEM containing 4500 mg/liter glucose, 10% FBS, 20 nM insulin, and 1 nM triiodothyronine. Fully confluent cells were incubated for 48 hr in differentiation medium supplemented with 0.5 mM isobutylmethylxanthine (IMBX), 0.5 μM dexamethasone and 0.125 mM indomethacin (induction medium). After 48 hr of induction, cells were maintained in differentiation medium for 5 days.

Dietary Studies

Five-week-old mice were housed four or five per cage and maintained on a fixed 12 hr light/dark cycle. The animals were fed regular chow diet (Teklad F6 S664, Harlan Tekland, Madison, WT) or high-fat diet (D12330, Research Diets, New Brunswick, NJ). The chow diet contained 27% kcal protein, 17% kcal fat, and 57% kcal carbohydrate. The high-fat diet contained 20% kcal protein, 60% kcal fat, and 20% kcal carbohydrate. The mice were kept on the diets for 12 weeks. They had free access to water and food.

Glucose Tolerance Test

Mice were fasted overnight (16 hr), and then 2 mg/g glucose was injected intraperitoneally. Blood glucose levels were measured using a One-Touch Ultra glucometer (LifeScan, Milpitas, CA) at 0, 15, 30, 60, and 120 min after glucose administration.

Biochemical Analysis

Mice were fasted overnight (16 hr). Blood samples were collected performance of heart punctures. Plasma samples were obtained by centrifuging blood in Microtainer plasma separator tubes (Becton Dickinson, Franklin Lakes, NJ). Plasma was assayed for insulin with an ultra sensitive mouse insulin ELISA kit (Crystal Chem, Downers Grove, IL). The measurements of blood cholesterol, β-hydroxybutyrate, FFA and triglycerides were performed by the Cincinnati Mouse Metabolic Phenotyping Center (MMPC).

Mitochondrial Preparation

Brown adipose tissue mitochondria were prepared as described previously (Shabalina et al., 2004). In brief, four Tyk2$^{+/+}$ and/or Tyk2$^{-/-}$ mice were sacrificed for each experiment. The interscapular brown adipose tissue depots were dissected out, cleaned from white adipose tissue and pooled in ice-cold isolation buffer (250 mM sucrose, 10 mM Tris-HCl, 1 mM EDTA, and 0.2% defatted BSA). The tissue was kept at 4°C throughout the isolation process. The tissue was minced with scissors, homogenized in a glass homogenizer with Teflon pestle, and centrifuged 8,500 × g for 10 min. The supernatant containing fat layer was discarded. The pellet was resuspended in isolation buffer and centrifuged at 500 × g for 10 min. The resulting supernatant was transferred to a clean tube and centrifuged again at 8500 × g for 10 min. The mitochondrial pellet was resuspended in KME buffer at pH 7.4 (100 mM KCl, 50 mM MOPS, 0.5 mM EGTA) and used within 4 hr after isolation. The protein concentration was measured with the Lowry method (with BSA as a standard and sodium deoxycholate as a detergent) (Lowry et al., 1951).

Oxygen Consumption

Oxygen consumption was measured with a Clark-type oxygen electrode (Strathkelvin Instruments, North Lanarkshire, UK) at 30°C in respiration buffer at pH 7.4 (100 mM KCl, 50 mM MOPS, 1 mM EGTA, 5 mM KH_2PO_4, and 0.1% defatted BSA). The mitochondrial suspension was continuously stirred in the chambers with magnetic stirrers. Oxygen consumption rates were measures in the presence of the substrate of interest: for complex I (5 mM pyruvate plus 5 mM malate), for complex II (20 mM succinate with 7.5 μM rotenone). Subsequently, 1 mM GDP and 0.2 mM dinitrophenol (DNP) were added.

Measurement of Energy Expenditure by Indirect Calorimetry

Metabolic rates were measured by indirect calorimetry in Tyk2$^{+/+}$ and Tyk2$^{-/-}$ mice by using an eight-chamber open-circuit Oxymax system (CLAMS, Columbus Instruments, Columbus, OH) at Mouse Metabolic Phenotyping Center in the Case Western Reserve University (Cleveland, Ohio). In brief, mice were individually housed in acrylic calorimeter chambers through which air of known O_2 concentration was passed at a constant flow rate. The system automatically withdrew gas samples from each chamber hourly for 24 hr. The system then calculated the volume of O_2 consumed (VO_2) and CO_2 generated (VCO_2) for each mouse in 1 hr normalized by lean body mass. Body composition of unanesthetized mice was measured by quantitative magnetic resonance imaging with EchoMRI (Echo Medical Systems, Houston, TX) as previously described (Lo et al., 2008). The RQ, ratio of the VCO_2 to VO_2, was calculated. Heat expenditures were measured throughout the study in light and dark cycles and under fed and fasting conditions and are represented in kcal/g/day. Mice were maintained at 25°C and had free access to water under all conditions.

RNA Extraction and Real-Time qPCR

Total RNA was isolated with TRI Reagent (Molecular Research, Cincinnati, OH), according to the manufacturer's instructions. Isolated RNA samples were treated with DNase (Promega, Madison, WI), Complementary DNA (cDNA) was synthesized from 2 μg RNA with the Tetro cDNA Synthesis Kit (Bioline, Taunton, MA), real-time qPCR was performed with the SensiMix SYBR and Fluorescein Kit (Bioline, Taunton, MA) according to manufacturer's instruction. All the samples were assayed in duplicates and analyzed with a CFX96 Real-Time PCR Detection System (Bio-Rad, Hercules, CA). Table S2 contains a full list of the primer sequences. Primers for Tyk2, Jak1, Jak2, OPA1, Mfn1, and Mfn2 were purchased from SuperArray (QIAGEN SABioscience, Frederick, MD).

Bisulfite Sequencing

Genomic DNA (1.5 μg) was converted with the EZ DNA methylation kit (Zymo Research, Orange, CA) according to the supplier's instructions. The treated DNA was amplified by PCR with the bisulfite-specific primers listed in Table S3. The amplification conditions for the 830 bp (Cidea promoter) and 730 bp (UCP1 promoter) DNA fragments were as follows: stage 1, 95°C/3 min/1 cycle; stage 2, 95°C/1 min/55°C/1 min/73°C/1 min/40 cycles; stage 3, 73°C/5 min/1 cycle. PCR products were cloned into the pCR2.1-TOPO vector (Invitrogen, Carlsbad, CA), and eight to 15 clones for each were picked and sequenced.

Chromatin Immunoprecipitation Assay

Immortalized Tyk2$^{+/+}$ and Tyk2$^{-/-}$ differentiated adipocytes were crosslinked with 1% formaldehyde for 10 min at 37°C and then washed with ice-cold PBS containing 125 mM glycine and 1 mM PMSF. Chromatin was sonicated and immunoprecipitated with specific antibodies exactly as described in the chromatin immunoprecipitation (ChIP) protocol provided by Upstate (Charlottesville, VA). The following antibodies were used: ChIPAb+ Trimethyl-Histone H3 (Lys4) from Milipore. The primers used in qPCR are listed in Table S4.

Statistical Analysis

Results are presented as the mean ± SEM. Statistical comparison was performed with a two-tailed Student's t test. While interpreting the data results a p value less than 0.05 was considered statistically significant and annotated by an asterisk.

SUPPLEMENTAL INFORMATION

Supplemental Information includes Supplemental Experimental Procedures, four figures, and four tables and can be found with this article online at http://dx.doi.org/10.1016/j.cmet.2012.11.005.

ACKNOWLEDGMENTS

This work was supported in part by R01 AI059710-01 and R21 AI088487 to A.C.L. B.S. was supported by the Austrian Science Fund (FWF SFB-F28). We would like to thank Dr. Bruce Spiegelman for his advice.

Received: July 3, 2012
Revised: October 1, 2012
Accepted: November 9, 2012
Published: December 4, 2012

REFERENCES

Chen, H., and Chan, D.C. (2010). Physiological functions of mitochondrial fusion. Ann. N Y Acad. Sci. *1201*, 21–25.

Cho, Y.-W., Hong, S., Jin, Q., Wang, L., Lee, J.-E., Gavrilova, O., and Ge, K. (2009). Histone methylation regulator PTIP is required for PPARgamma and C/EBPalpha expression and adipogenesis. Cell Metab. *10*, 27–39.

Cypess, A.M., Lehman, S., Williams, G., Tal, I., Rodman, D., Goldfine, A.B., Kuo, F.C., Palmer, E.L., Tseng, Y.H., Doria, A., et al. (2009). Identification and importance of brown adipose tissue in adult humans. N. Engl. J. Med. *360*, 1509–1517.

Dawson, M.A., Bannister, A.J., Göttgens, B., Foster, S.D., Bartke, T., Green, A.R., and Kouzarides, T. (2009). JAK2 phosphorylates histone H3Y41 and excludes HP1alpha from chromatin. Nature *461*, 819–822.

Decker, T., Lew, D.J., and Darnell, J.E.J., Jr. (1991). Two distinct alpha-interferon-dependent signal transduction pathways may contribute to activation of transcription of the guanylate-binding protein gene. Mol. Cell. Biol. *11*, 5147–5153.

Dlasková, A., Clarke, K.J., and Porter, R.K. (2010). The role of UCP 1 in production of reactive oxygen species by mitochondria isolated from brown adipose tissue. Biochim. Biophys. Acta *1797*, 1470–1476.

Fasshauer, M., Klein, J., Ueki, K., Kriauciunas, K.M., Benito, M., White, M.F., and Kahn, C.R. (2000). Essential role of insulin receptor substrate-2 in insulin stimulation of Glut4 translocation and glucose uptake in brown adipocytes. J. Biol. Chem. *275*, 25494–25501.

Imai, T., Jiang, M., Chambon, P., and Metzger, D. (2001). Impaired adipogenesis and lipolysis in the mouse upon selective ablation of the retinoid X receptor alpha mediated by a tamoxifen-inducible chimeric Cre recombinase (Cre-ERT2) in adipocytes. Proc. Natl. Acad. Sci. USA *98*, 224–228.

Jung, J.E., Lee, H.G., Cho, I.H., Chung, D.H., Yoon, S.H., Yang, Y.M., Lee, J.W., Choi, S., Park, J.W., Ye, S.K., and Chung, M.H. (2005). STAT3 is a potential modulator of HIF-1-mediated VEGF expression in human renal carcinoma cells. FASEB J. *19*, 1296–1298.

Karamanlidis, G., Karamitri, A., Docherty, K., Hazlerigg, D.G., and Lomax, M.A. (2007). C/EBPbeta reprograms white 3T3-L1 preadipocytes to a Brown adipocyte pattern of gene expression. J. Biol. Chem. *282*, 24660–24669.

Karamitri, A., Shore, A.M., Docherty, K., Speakman, J.R., and Lomax, M.A. (2009). Combinatorial transcription factor regulation of the cyclic AMP-response element on the Pgc-1alpha promoter in white 3T3-L1 and brown HIB-1B preadipocytes. J. Biol. Chem. *284*, 20738–20752.

Klöting, N., Koch, L., Wunderlich, T., Kern, M., Ruschke, K., Krone, W., Brüning, J.C., and Blüher, M. (2008). Autocrine IGF-1 action in adipocytes controls systemic IGF-1 concentrations and growth. Diabetes *57*, 2074–2082.

Lidell, M.E., Seifert, E.L., Westergren, R., Heglind, M., Gowing, A., Sukonina, V., Arani, Z., Itkonen, P., Wallin, S., Westberg, F., et al. (2011). The adipocyte-expressed forkhead transcription factor Foxc2 regulates metabolism through altered mitochondrial function. Diabetes *60*, 427–435.

Lo, C.M., Samuelson, L.C., Chambers, J.B., King, A., Heiman, J., Jandacek, R.J., Sakai, R.R., Benoit, S.C., Raybould, H.E., Woods, S.C., and Tso, P. (2008). Characterization of mice lacking the gene for cholecystokinin. Am. J. Physiol. Regul. Integr. Comp. Physiol. *294*, R803–R810.

Lowry, O.H., Rosebrough, N.J., Farr, A.L., and Randall, R.J. (1951). Protein measurement with the Folin phenol reagent. J. Biol. Chem. *193*, 265–275.

Mao, C., Davies, D., Kerr, I.M., and Stark, G.R. (1993). Mutant human cells defective in induction of major histocompatibility complex class II genes by interferon gamma. Proc. Natl. Acad. Sci. USA *90*, 2880–2884.

Mesaros, A., Koralov, S.B., Rother, E., Wunderlich, F.T., Ernst, M.B., Barsh, G.S., Rajewsky, K., and Brüning, J.C. (2008). Activation of Stat3 signaling in AgRP neurons promotes locomotor activity. Cell Metab. *7*, 236–248.

Nedergaard, J., Bengtsson, T., and Cannon, B. (2007). Unexpected evidence for active brown adipose tissue in adult humans. Am. J. Physiol. Endocrinol. Metab. *293*, E444–E452.

Nie, Y., Erion, D.M., Yuan, Z., Dietrich, M., Shulman, G.I., Horvath, T.L., and Gao, Q. (2009). STAT3 inhibition of gluconeogenesis is downregulated by SirT1. Nat. Cell Biol. *11*, 492–500.

O'Brien, P.E., Dixon, J.B., Laurie, C., and Anderson, M. (2005). A prospective randomized trial of placement of the laparoscopic adjustable gastric band: comparison of the perigastric and pars flaccida pathways. Obes. Surg. *15*, 820–826.

Ohno, H., Shinoda, K., Spiegelman, B.M., and Kajimura, S. (2012). PPARγ agonists induce a white-to-brown fat conversion through stabilization of PRDM16 protein. Cell Metab. *15*, 395–404.

Pearse, R.N., Feinman, R., and Ravetch, J.V. (1991). Characterization of the promoter of the human gene encoding the high-affinity IgG receptor: transcriptional induction by gamma-interferon is mediated through common DNA response elements. Proc. Natl. Acad. Sci. USA *88*, 11305–11309.

Ragimbeau, J., Dondi, E., Vasserot, A., Romero, P., Uzé, G., and Pellegrini, S. (2001). The receptor interaction region of Tyk2 contains a motif required for its nuclear localization. J. Biol. Chem. *276*, 30812–30818.

Raz, R., Durbin, J.E., and Levy, D.E. (1994). Acute phase response factor and additional members of the interferon-stimulated gene factor 3 family integrate diverse signals from cytokines, interferons, and growth factors. J. Biol. Chem. *269*, 24391–24395.

Russell, A.P., Crisan, M., Léger, B., Corselli, M., McAinch, A.J., O'Brien, P.E., Cameron-Smith, D., Péault, B., Casteilla, L., and Giacobino, J.P. (2012). Brown adipocyte progenitor population is modified in obese and diabetic skeletal muscle. Int J Obes (Lond) *36*, 155–158.

Saito, M., Okamatsu-Ogura, Y., Matsushita, M., Watanabe, K., Yoneshiro, T., Nio-Kobayashi, J., Iwanaga, T., Miyagawa, M., Kameya, T., Nakada, K., et al. (2009). High incidence of metabolically active brown adipose tissue in healthy adult humans: effects of cold exposure and adiposity. Diabetes *58*, 1526–1531.

Sanchez-Gurmaches, J., Hung, C.M., Sparks, C.A., Tang, Y., Li, H., and Guertin, D.A. (2012). PTEN loss in the Myf5 lineage redistributes body fat and reveals subsets of white adipocytes that arise from Myf5 precursors. Cell Metab. *16*, 348–362.

Schulz, T.J., Huang, T.L., Tran, T.T., Zhang, H., Townsend, K.L., Shadrach, J.L., Cerletti, M., McDougall, L.E., Giorgadze, N., Tchkonia, T., et al. (2011). Identification of inducible brown adipocyte progenitors residing in skeletal muscle and white fat. Proc. Natl. Acad. Sci. USA *108*, 143–148.

Seale, P., Kajimura, S., Yang, W., Chin, S., Rohas, L.M., Uldry, M., Tavernier, G., Langin, D., and Spiegelman, B.M. (2007). Transcriptional control of brown fat determination by PRDM16. Cell Metab. *6*, 38–54.

Seale, P., Bjork, B., Yang, W., Kajimura, S., Chin, S., Kuang, S., Scimè, A., Devarakonda, S., Conroe, H.M., Erdjument-Bromage, H., et al. (2008). PRDM16 controls a brown fat/skeletal muscle switch. Nature *454*, 961–967.

Shabalina, I.G., Jacobsson, A., Cannon, B., and Nedergaard, J. (2004). Native UCP1 displays simple competitive kinetics between the regulators purine nucleotides and fatty acids. J. Biol. Chem. *279*, 38236–38248.

Shaw, M.H., Boyartchuk, V., Wong, S., Karaghiosoff, M., Ragimbeau, J., Pellegrini, S., Muller, M., Dietrich, W.F., and Yap, G.S. (2003). A natural mutation in the Tyk2 pseudokinase domain underlies altered susceptibility of B10.Q/J mice to infection and autoimmunity. Proc. Natl. Acad. Sci. USA *100*, 11594–11599.

Shimoda, K., Kato, K., Aoki, K., Matsuda, T., Miyamoto, A., Shibamori, M., Yamashita, M., Numata, A., Takase, K., Kobayashi, S., et al. (2000). Tyk2 plays a restricted role in IFN alpha signaling, although it is required for IL-12-mediated T cell function. Immunity *13*, 561–571.

Shore, A., Karamitri, A., Kemp, P., Speakman, J.R., and Lomax, M.A. (2010). Role of Ucp1 enhancer methylation and chromatin remodelling in the control of Ucp1 expression in murine adipose tissue. Diabetologia *53*, 1164–1173.

Stark, G.R., Kerr, I.M., Williams, B.R.G., Silverman, R.H., and Schreiber, R.D. (1998). How cells respond to interferons. Annu. Rev. Biochem. *67*, 227–264.

Strobl, B., Stoiber, D., Sexl, V., and Mueller, M. (2011). Tyrosine kinase 2 (TYK2) in cytokine signalling and host immunity. Front. Biosci. *16*, 3214–3232.

Tseng, Y.H., Kriauciunas, K.M., Kokkotou, E., and Kahn, C.R. (2004). Differential roles of insulin receptor substrates in brown adipocyte differentiation. Mol. Cell. Biol. *24*, 1918–1929.

Urs, S., Harrington, A., Liaw, L., and Small, D. (2006). Selective expression of an aP2/Fatty Acid Binding Protein 4-Cre transgene in non-adipogenic tissues during embryonic development. Transgenic Res. *15*, 647–653.

Virtanen, K.A., Lidell, M.E., Orava, J., Heglind, M., Westergren, R., Niemi, T., Taittonen, M., Laine, J., Savisto, N.J., Enerbäck, S., and Nuutila, P. (2009). Functional brown adipose tissue in healthy adults. N. Engl. J. Med. *360*, 1518–1525.

Yang, J., Huang, J., Dasgupta, M., Sears, N., Miyagi, M., Wang, B., Chance, M.R., Chen, X., Du, Y., Wang, Y., et al. (2010). Reversible methylation of promoter-bound STAT3 by histone-modifying enzymes. Proc. Natl. Acad. Sci. USA *107*, 21499–21504.

Zick, M., Rabl, R., and Reichert, A.S. (2009). Cristae formation-linking ultrastructure and function of mitochondria. Biochim. Biophys. Acta *1793*, 5–19.

Zingaretti, M.C., Crosta, F., Vitali, A., Guerrieri, M., Frontini, A., Cannon, B., Nedergaard, J., and Cinti, S. (2009). The presence of UCP1 demonstrates that metabolically active adipose tissue in the neck of adult humans truly represents brown adipose tissue. FASEB J. *23*, 3113–3120.